



## Using polarization analysis to separate the coherent and incoherent scattering from protein samples

Ana M. Gaspar<sup>a,b,\*</sup>, Sebastian Busch<sup>a,b</sup>, Marie-Sousai Appavou<sup>a,c</sup>, Wolfgang Haeussler<sup>b,d</sup>, Robert Georgii<sup>b,d</sup>, Yixi Su<sup>c</sup>, Wolfgang Doster<sup>a</sup>

<sup>a</sup> Physik Department E13, Technische Universität München, Germany

<sup>b</sup> Forschungsneutronenquelle Heinz Maier-Leibnitz (FRM II), Technische Universität München, Germany

<sup>c</sup> Forschungszentrum Jülich GmbH, Institut für Festkörperforschung, Jülich Center for Neutron Science at FRM II Outstation, Germany

<sup>d</sup> Physik Department E21, Technische Universität München, Germany

### ARTICLE INFO

#### Article history:

Received 13 March 2009

Received in revised form 29 June 2009

Accepted 30 June 2009

Available online 10 July 2009

#### Keywords:

Neutron scattering

Polarization analysis

Coherent/incoherent nuclear scattering

Protonated/deuterated protein

Structure

Dynamic

### ABSTRACT

Polarization analysis was used to separate experimentally the coherent and spin-incoherent nuclear static scattering functions, from a representative set of samples of interest for protein studies. This method had so far limited application in the study of amorphous materials, despite the relevance of the information that it provides. It allows, for instance, the experimental determination of the structure factor of materials containing a significant amount of hydrogen atoms, avoiding the contamination of measurements by a non-negligible incoherent background. Knowledge of the relative importance of the coherent and incoherent terms at different  $Q$ -values is also a pre-requisite for the interpretation of quasielastic neutron scattering experiments, performed at instruments in which the total dynamic scattering function is measured, such as conventional time-of-flight and backscattering spectrometers. Combining data from different instruments, it was possible to cover a wide  $Q$ -range, from the small-angle region ( $0.006 < Q < 0.04 \text{ \AA}^{-1}$ ) to the wide-angle region (up to  $\approx 2.35 \text{ \AA}^{-1}$ ). Quantitative information was obtained on the fraction of coherent to spin-incoherent scattering from different protein samples: deuterated and protonated protein powders at different hydration levels and solutions of protonated proteins in  $D_2O$  at different concentrations. The results obtained are discussed in the context of the validity of the assumptions generally made when interpreting quasielastic neutron scattering experiments performed without polarization analysis.

© 2009 Elsevier B.V. All rights reserved.

### 1. Introduction

It is known that the scattering of cold and thermal neutrons by nuclei depends on the relative orientation of the neutron and nucleus spins [1–3]. In the case of a sample with randomly oriented nuclear spins, it can be decomposed into an incoherent nuclear scattering term and a coherent nuclear scattering term, each of these terms providing information on different dynamical processes. The incoherent term contains information exclusively on the so-called self correlation function (the correlation between the positions of the same atom at different time instants) and hence on the dynamics of the individual atoms, whereas the coherent term also contains information on the so-called pair correlation function (the correlation between the positions of different atoms at different time instants) and hence on the collective dynamics, as well as on the average relative position of the different atoms (structural information). These two types of dynamical processes

are intrinsically distinct and give, therefore, rise to distinct neutron scattering functions [4–6].

Neutron scattering instruments dedicated to dynamical investigations generally measure the total scattering function, which greatly hampers the interpretation of the results obtained for samples having coherent and incoherent scattering terms of similar order of magnitude. This is unfortunately frequently the case for diffuse scattering samples, like liquids and soft-matter systems, since they are largely amorphous, with broad structure factor peaks extending over a large  $Q$ -range, instead of well-defined Bragg peaks.

Polarization analysis has been known to provide the means to separate experimentally the coherent and spin-incoherent terms of the neutron scattering function, as coherent neutron scattering events are scattering events which do not involve a flip of the neutron spin, whereas only 1/3 of the spin-incoherent neutron scattering events of a sample with randomly oriented nuclei spins are without spin-flip, the other 2/3 being with spin-flip [7–9]. Isotope incoherent scattering, which results from the same atomic position being possibly occupied in different molecules by different isotopes of the same element, also occurs without neutron spin-flip. Nevertheless, whenever this last term can be neglected, the separation of the coherent and the

\* Corresponding author. Physik Department E13, Technische Universität München, Germany. Tel.: +49 15204632596.

E-mail address: [ana.gaspar@frm2.tum.de](mailto:ana.gaspar@frm2.tum.de) (A.M. Gaspar).

incoherent nuclear scattering processes can be simply achieved using a polarized incident neutron beam and counting separately the neutrons scattered with and without spin-flip with regard to the incident beam polarization.

This method had, however, so far very limited application in the study of amorphous diffuse scattering materials, probably mainly due to the technical difficulties related to the intensity costs inherent to a setup allowing for polarization analysis. The few works published up to now [10–13] consist mainly of a proof of principle, which found little or no continuation in the different fields of liquid and soft condensed matter investigations, despite of the relevance of the information that can be possibly obtained. Instead, some fields of research, among which the one dedicated to the study of proteins by neutron scattering [14], continue to base the interpretation of dynamical measurements performed at instruments in which the total scattering function is measured on assumptions such as the one that the coherent term is negligible. Although systematically invoked in quasielastic neutron scattering investigations (e.g. [15]), the validity of this assumption, over the entire  $Q$ -range nowadays accessed by time-of-flight or backscattering instruments, is by no means evident. On the other hand, in small-angle scattering investigations, it is the incoherent scattering term that is systematically assumed to be flat and negligible over the entire  $Q$ -range of the acquisitions, even though the high-angle limit of these acquisitions has been continuously increasing.

The instrumentation developments of the last decades should have brought neutron flux values to a level allowing to dispense these data analysis assumptions and to obtain experimental information of good statistical quality on the  $Q$ -dependent fraction of coherent to incoherent scattering from diffuse scattering samples. Here we present results of such attempts performed recently on different samples of interest to the community studying proteins by neutron scattering. These are results from static scattering measurements performed with polarization analysis at two different instruments installed at the FRM II neutron facility, MIRA [16] and DNS [17], and covering a wide  $Q$ -range from the small-angle region ( $0.006 < Q < 0.04 \text{ \AA}^{-1}$ ), where scattering from a protein solution is believed to be dominated by the coherent term, to the wide-angle region (up to  $Q \approx 2.35 \text{ \AA}^{-1}$ ) usually explored in quasielastic neutron scattering measurements under the assumption that it is the incoherent term that dominates. To our knowledge, these are the first results of this type to be published on protein samples.

## 2. Materials and methods

### 2.1. Samples

Three proteins have been used in the investigations reported here, namely protonated horse heart myoglobin and protonated haemoglobin with their labile hydrogen atoms exchanged by deuterium atoms and per-deuterated C-phycoyanin with its labile deuterium atoms exchanged by hydrogen. A full set of samples was then prepared, consisting of protonated and deuterated protein powder samples (dry and hydrated), as well as solutions of the protonated proteins in  $D_2O$  at different concentrations, ranging from dilute solutions (5 mg/ml), generally used in small-angle scattering experiments, to very concentrated solutions (360 mg/ml), covering the range generally used in time-of-flight or backscattering experiments. The composition, total coherent and incoherent scattering cross sections, and total transmission of the protein samples investigated are listed in Table 1.

The preparation of the protein powder samples involved dissolution of the dialyzed protein powders either in  $D_2O$ , in the case of myoglobin and haemoglobin, or in  $H_2O$ , in the case of C-phycoyanin, to allow for the exchange of the protein labile hydrogen or deuterium

**Table 1**

Composition, total coherent and incoherent scattering cross sections, and total transmission of the protein samples investigated.

Protonated proteins (H → D exchanged)	$n$ $D_2O$ /protein	$\sigma_{coh}/\sigma_{tot}$	$\sigma_{inc}/\sigma_{tot}$	Trans.
<b>Haemoglobin</b>				
$(D_{920}H_{3452}C_{2818}N_{764}O_{786}S_{12}Fe_4)$				
$D_2O$ solution 250 mg/ml	11265	0.39	0.61	0.88
<b>Myoglobin</b>				
$(D_{274}H_{981}C_{783}N_{214}O_{222}S_2Fe_1)$				
D-dry powder	0	0.12	0.88	0.88
D-hyd powder 0.35 g/g	313	0.16	0.84	0.88
D-hyd powder 0.74 g/g	648	0.20	0.80	0.87
$D_2O$ solution 360 mg/ml	1991	0.32	0.68	0.78
$D_2O$ solution 200 mg/ml	4170	0.44	0.56	0.83
$D_2O$ solution 100 mg/ml	9071	0.56	0.44	0.88
$D_2O$ solution 50 mg/ml	18873	0.66	0.34	0.89
$D_2O$ solution 20 mg/ml	48289	0.73	0.27	0.90
$D_2O$ solution 10 mg/ml	97290	0.76	0.24	0.90
$D_2O$ solution 5 mg/ml	195311	0.77	0.23	0.90
$D_2O$	"∞"	0.79	0.21	0.90
Deuterated protein (D → H exchanged)	$n$ $H_2O$ /protein	$\sigma_{coh}/\sigma_{tot}$	$\sigma_{inc}/\sigma_{tot}$	Trans.
<b>C-phycoyanin</b>				
$(H_{568}D_{1879}C_{1540}N_{423}O_{488}S_{13})$				
H-dry powder	0	0.35	0.65	0.90
H-hyd powder 0.33 g/g	676	0.17	0.83	0.90

$n$  refers to the number of solvent molecules per protein molecule. Cross sections fractions calculated taking into account the cross sections for the elements and their isotopes tabulated by NIST [18]. Transmission values obtained with FRIDA [19] for the sample amounts in the beam.

atoms by the solvent isotopic species. Such a procedure rendered negligible the only possible source of isotope incoherent scattering in our samples. In fact, the isotopic composition of the naturally occurring atomic elements composing the proteins, and the purity of the solvent employed in the production of a per-deuterated protein, are such that no isotope incoherent scattering is expected to come from the protein non-exchangeable atoms [18]. Hence, for this type of samples, the only possibly relevant source of isotope incoherent scattering would be a non-complete exchange of the protein hydrogen or deuterium labile atoms by the solvent isotopic species (whenever the latter is different from the former), with an interchangeable mixture of H and D atoms remaining present in the sample.

After the exchange process, the dry powders were obtained by freeze-drying. The dryness of the powders was confirmed by further exposing these dry powders for long periods to high vacuum conditions, after which no further reduction of their masses was observed. The hydrated powders were obtained rehydrating the dry powders by vapour adsorption of  $D_2O$  or  $H_2O$ , up to the hydration levels required. The water content of the samples was determined by weighing. This was done not only before exposure to the neutron beam, but also controlled afterwards to exclude the possibility of dehydration during data acquisition.

The solution samples were obtained dissolving the protonated protein powders in  $D_2O$ . In the case of the highest concentration solutions, the final concentration level was achieved by centrifugation of a less concentrated solution using centricon filters from Millipore with a 3 kDa molecular weight cutoff. The concentration of all the solutions was further controlled by removing and subsequently drying small volumes of sample, weighing the resultant amounts of dry protein.

### 2.2. Measurements

Experiments covering the  $Q$ -range  $0.006 < Q < 0.4 \text{ \AA}^{-1}$  were performed at the MIRA instrument at the FRM II neutron facility, which

employs a supermirror for the polarization of the neutron incident beam [16]. Two alternative instrument configurations with regard to the polarization analyzer and detection system were used in order to maximize the signal to background ratio over the angular ranges of interest. The first setup (setup 1) involved the use of a quartz cell filled with polarized  $^3\text{He}$  gas, as analyzer, and a 2D position sensitive detector, while the second setup (setup 2) involved the use of a supermirror analyzer and a finger detector of 2.54 cm circular section. In both cases, a  $\pi$  spin flipper (of efficiency determined to be  $\sim 1$ ) was introduced before the sample to reverse the polarization of the  $\lambda = 9.75 \text{ \AA}$  incident neutron beam for spin-flip and non-spin-flip measurements. For setup 1, the total flipping ratio was decreasing in time, due to the ongoing depolarization of the  $^3\text{He}$  gas ( $R \sim 12 \rightarrow 6$ , over a period of 24 h), while in the case of setup 2, the total flipping ratio was determined to be  $R \sim 11.5$ . Setup 1 was used to explore the small-angle region ( $0.006 < Q < 0.04 \text{ \AA}^{-1}$ ), with the 2D-detector placed in the forward direction, while setup 2 was found to be the best option to explore the higher angular region ( $0.04 < Q < 0.4 \text{ \AA}^{-1}$ ).

Experiments covering the  $Q$ -range  $0.15 < Q < 2.35 \text{ \AA}^{-1}$  were performed at the DNS instrument of the Jülich Center for Neutron Science (FZ-J GmbH) now installed at the FRM II neutron facility [17]. It is a compact multi-detector instrument, covering the scattering angle range  $6^\circ < 2\theta < 125^\circ$  and employing focusing supermirrors both for the polarization of the incident beam, and for the analysis of the polarization of the scattered neutrons before the detector banks. Measurements were made in diffraction mode employing  $\lambda = 4.74 \text{ \AA}$  incident neutrons and, once again, a  $\pi$  spin flipper (of efficiency  $\sim 1$ ) was used before the sample to reverse the polarization of the incident beam in standard  $z$ -polarization analysis mode, measuring the spin-flip and non-spin-flip scattering intensities. Under the measuring conditions, the instrument flipping ratio was determined to be  $R \sim 25$  from measurements performed on a vanadium sample (a nearly 100% spin-incoherent scattering sample in this  $Q$ -range).

All samples were studied at room temperature (293 K) either in plane-parallel quartz cells of 1 mm sample thickness (MIRA), or in hollow cylinder aluminum containers defining a sample layer thickness of 0.5 mm (DNS). This choice of sample container geometry and sample thicknesses allowed for the best exploitation of the geometries and angular ranges available at each of the instruments, while keeping the sample transmission high (Table 1), thereby rendering the effects of multiple scattering negligible [20]. Measurements were also performed, under the same conditions, of pure  $\text{D}_2\text{O}$ , of the empty container, of a “black” sample (absorbing 100% of the neutrons going through the sample section), and of a vanadium sample having the same geometry and thickness as the samples.

The average acquisition time required for a good quality sample measurement at DNS was of about 6 h, for a  $\approx 10\%$  scattering sample (see Table 1). This corresponded to  $\approx 500$  mg of protein being placed in the beam for each of the protonated protein powder samples, as well as for the hydrated powder of the deuterated protein, and to the double of that amount in the case of the dry deuterated powder. In the case of the liquid samples, the volume investigated at DNS was in all cases 2.5 ml.

### 2.3. Data-reduction and analysis

The one dimensional non-spin-flip (NSF) and spin-flip (SF) scattered intensities were obtained either by radial averaging the 2D scattering rings detected at setup 1 of MIRA, or directly as detector counts versus detector angular position for setup 2 of MIRA and for DNS. These intensities were then normalized to the monitor counts and the sample signals,  $I_{\text{NSFm}}(Q)$  and  $I_{\text{SFm}}(Q)$ , were obtained by subtraction of the empty can and black sample signals taking into account the appropriate self-absorption corrections [19,21,22].

Intensities were then corrected for the finite instrument flipping ratio  $R$  [23]:

$$\begin{cases} I_{\text{NSFc}}(Q) = I_{\text{NSFm}}(Q) + \frac{1}{R-1}(I_{\text{NSFm}}(Q) - I_{\text{SFm}}(Q)) \\ I_{\text{SFc}}(Q) = I_{\text{SFm}}(Q) + \frac{1}{R-1}(I_{\text{SFm}}(Q) - I_{\text{NSFm}}(Q)) \end{cases} \quad (1)$$

after which the coherent and incoherent terms were obtained:

$$\begin{cases} I_{\text{coh}}(Q) = I_{\text{NSFc}}(Q) - \frac{1}{2}I_{\text{SFc}}(Q) \\ I_{\text{inc}}(Q) = \frac{3}{2}I_{\text{SFc}}(Q) \end{cases} \quad (2)$$

The last step, taken in the case of the DNS data, was to use the incoherent scattering term as an internal calibration factor to normalize the coherent term [24]. Hence, calculating  $\alpha$  as:

$$\alpha = \frac{I_{\text{coh}}(Q)}{I_{\text{inc}}(Q)} \quad (3)$$

the coherent and incoherent terms of the scattering function were obtained as:

$$\begin{cases} S_{\text{coh}}(Q) = \frac{\sigma_{\text{inc}}}{\sigma_{\text{tot}}} \alpha \\ S_{\text{inc}}(Q) = \frac{\sigma_{\text{inc}}}{\sigma_{\text{tot}}} \end{cases} \quad (4)$$

and the  $Q$ -dependent fractions of coherent and incoherent scattering events as:

$$\begin{cases} \frac{S_{\text{coh}}(Q)}{S_{\text{tot}}(Q)} = \frac{\alpha}{1 + \alpha} \\ \frac{S_{\text{inc}}(Q)}{S_{\text{tot}}(Q)} = \frac{1}{1 + \alpha} \end{cases} \quad (5)$$

Such a procedure has the further advantages of cancelling, through  $\alpha$ , any other possible instrumental effects (detector dependent efficiency, geometrical factors, etc.) not previously accounted for, as well as of cancelling the Debye–Waller factor and accounting for the inelasticity corrections, all of these affecting in a similar way the spin-flip and non spin-flip scattered intensities.

## 3. Results and discussion

Fig. 1 illustrates, for some of the protein solutions investigated, how polarization analysis allowed the successful separation of the coherent and incoherent terms of the static structure factors, over the different  $Q$ -ranges accessed by the different instrumental setups used. In all three situations, the incoherent term appears, as expected, as a flat featureless term, while the coherent term changes significantly with  $Q$ , exhibiting the expected behavior both in the small-angle region (a), where a fast decay with  $Q$  is observed, as well as in the intermediate (b) to wide-angle (c) regions, where coherent peaks, related to either the protein–protein distances within the solution (at about  $0.10$ – $0.15 \text{ \AA}^{-1}$ ), or to typical intramolecular helix–helix distances within the protein (around  $0.7 \text{ \AA}^{-1}$ ) and to the solvent–solvent characteristic distances (around  $2.0 \text{ \AA}^{-1}$ ) are clearly visible.

These results also demonstrate, for these solutions, the clear predominance of a coherent term which is at least one order of magnitude more intense than the incoherent term in the small-angle scattering region (Fig. 1a). For higher  $Q$ -values the decaying coherent intensities become of the same order of magnitude as the incoherent term, with a crossover from mainly coherent to mainly incoherent scattering around  $0.25$ – $0.30 \text{ \AA}^{-1}$  (Fig. 1b, c). The situation of a clear

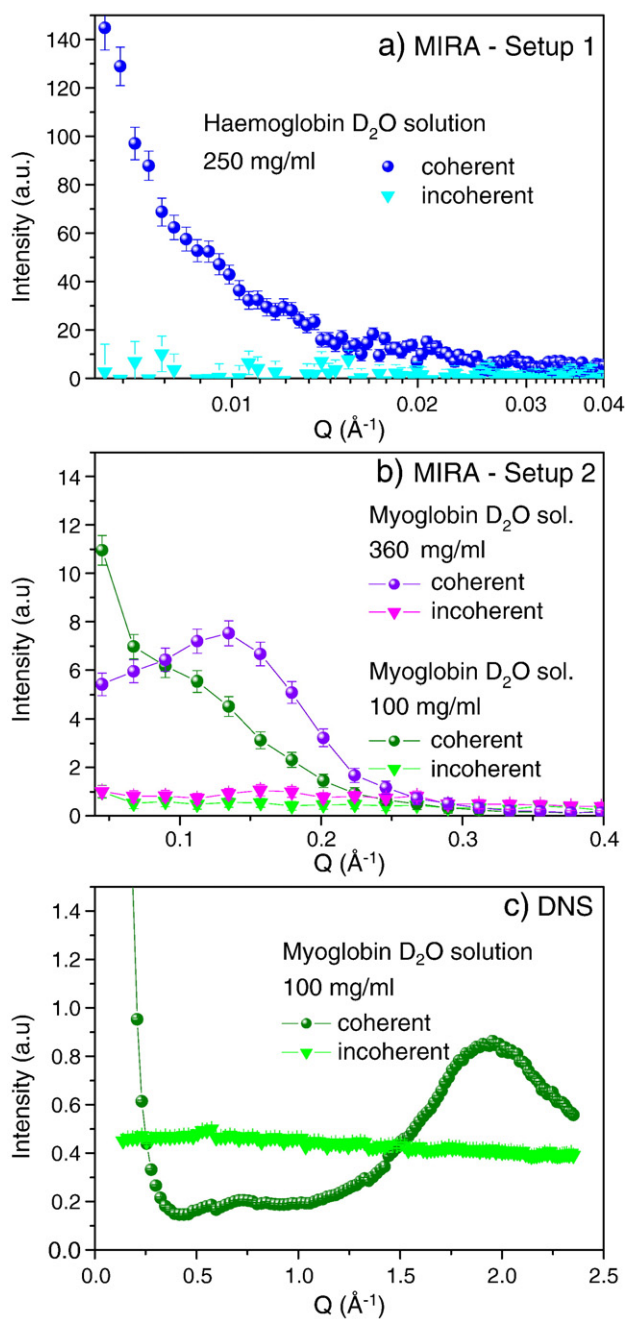


**Fig. 1.** Coherent and incoherent scattering intensities obtained over different intensity and  $Q$ -ranges using three different instrument setups: (a) setup 1 at MIRA: small-angle scattering region ( $0.006 < Q < 0.04 \text{ \AA}^{-1}$ ); (b) setup 2 at MIRA: intermediate scattering region ( $0.04 < Q < 0.4 \text{ \AA}^{-1}$ ); (c) DNS: intermediate to wide-angle scattering region ( $0.15 < Q < 2.35 \text{ \AA}^{-1}$ ).

predominance of the incoherent term, however, never observed, the two terms playing alternating roles for  $Q > 0.3 \text{ \AA}^{-1}$  due to the oscillations of the structure factor (Fig. 1c).

In the following, detailed attention will be given to the region  $0.15 < Q < 2.35 \text{ \AA}^{-1}$ , for which data of good statistical quality were obtained at the DNS instrument (Fig. 1c), and where, as will be seen, for most of the samples the coherent term comes underneath the incoherent term, while still exhibiting significant oscillations. This is also the  $Q$ -range usually accessed by time-of-flight and backscattering spectrometers, the results being therefore relevant for the interpretation of many of the information on protein and protein hydration water dynamics obtained at such instruments.

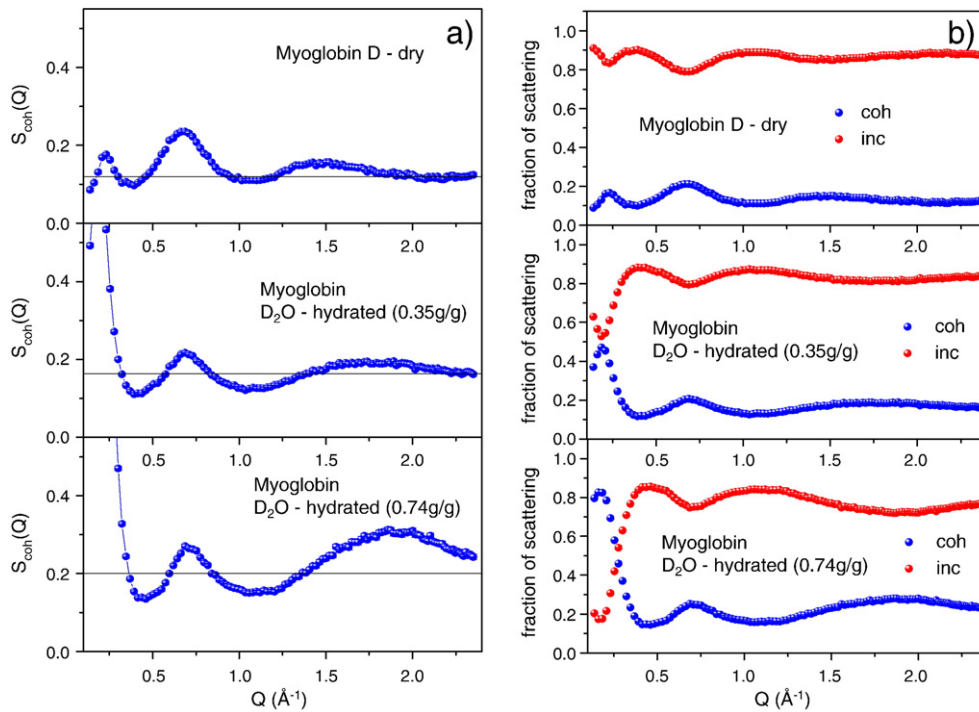
### 3.1. Powders and solutions of protonated myoglobin in $D_2O$

Fig. 2 depicts the results obtained for the myoglobin powders investigated, while Fig. 3 exhibits the same information for three of the solutions of myoglobin in  $D_2O$  investigated, with concentrations ranging from 5 mg/ml to 360 mg/ml (see Table 1). These comprise the coherent structure factors, displayed on the left-hand side of the figures (a), as well as the  $Q$ -dependent fractions of coherent and incoherent scattering events, displayed on the right-hand side of the figures (b), corresponding to the three quantities defined by expressions (4) and (5) presented above.

The coherent structure factors (a) exhibit maxima and minima consistent with the results previously obtained for amorphous myoglobin samples from diffraction experiments performed without polarization analysis [25]. In the case of the dry myoglobin powder, three interference maxima (at  $0.23 \text{ \AA}^{-1}$ ,  $0.65 \text{ \AA}^{-1}$  and  $1.4 \text{ \AA}^{-1}$ ) corresponding to characteristic inter and intra protein distances [26] can be clearly distinguished, even though the coherent term represents only between 10% and 20% of the total scattering over this  $Q$ -range. For the hydrated powders, an intensity increase in the small-angle region is observed, as a result of the formation of a layer of  $D_2O$  molecules around the protein which has a scattering length considerably distinct from that of the protein, therefore enhancing the contrast between the protein and its environment. Differences with regard to the dry powder are also observed in the region  $1.5\text{--}2.3 \text{ \AA}^{-1}$  due to the existence of new positional correlations between the solvent molecules and the protein outer atoms, as well as between the solvent molecules themselves. These latter positional correlations give rise, in the bulk solvent [27,28], to a broad peak around  $2.0 \text{ \AA}^{-1}$  which becomes of increasing importance as the protein concentration decreases when going from the powders (Fig. 2a) to the protein solutions (Fig. 3a).

As for the  $Q$ -dependent fractions of coherent and incoherent scattering events, displayed on the right-hand side (b), the importance of the contributions oscillates, as expected, around the tabulated  $\sigma_{\text{coh}}/\sigma_{\text{tot}}$  and  $\sigma_{\text{inc}}/\sigma_{\text{tot}}$  values (listed in Table 1). These oscillations increase in amplitude with increasing  $D_2O$  content of the samples due to the increase in coherent scattering cross section. For the dry powder, the percentage of incoherent scattering events varies only between 79% and 91% of the total scattering over the entire  $Q$ -range investigated, whereas for the hydrated powders bigger changes are observed, specially for  $Q < 0.35 \text{ \AA}^{-1}$  (Fig. 2b). It is particularly noteworthy that for the powder of 0.74 g/g hydration the scattering is even predominantly coherent for any  $Q$ -value below  $0.28 \text{ \AA}^{-1}$ , the percentage of coherent scattering events reaching a level as high as 80% already at  $Q = 0.18 \text{ \AA}^{-1}$ . Nevertheless, for  $Q > 0.35 \text{ \AA}^{-1}$ , the fractions of coherent and incoherent scattering events still follow the tabulated values  $\sigma_{\text{coh}}/\sigma_{\text{tot}}$  and  $\sigma_{\text{inc}}/\sigma_{\text{tot}}$ , with only relatively small oscillations: namely, the percentage of incoherent scattering events varies between 88% and 80% of the total scattering for the 0.34 g/g hydrated sample and between 85% and 72% for the 0.74 g/g hydrated sample over the  $Q$ -range investigated.

Bigger variations are observed for the aqueous solutions (Fig. 3b), for which a first crossover from mainly coherent to mainly incoherent scattering is observed in the small-angle region at  $Q$ -values between  $0.18$  and  $0.26 \text{ \AA}^{-1}$ , depending on the protein concentration. A second crossover, this time from mainly incoherent to mainly coherent, is then also observed for all the solutions investigated with the exception of the most concentrated solution (Fig. 3a, top), at  $Q$ -values between  $1.1$  and  $1.7 \text{ \AA}^{-1}$  depending on the protein concentration, due to the rising solvent structure factor peak. Conversely, in the intermediate  $Q$ -range the percentage of incoherent scattering events supersedes the tabulated  $\sigma_{\text{inc}}/\sigma_{\text{tot}}$  values, reaching levels of about 80% in the case of the 360 mg/ml solution and 70% in the case of the 100 mg/ml solution and 60% in the case of the most diluted solution.

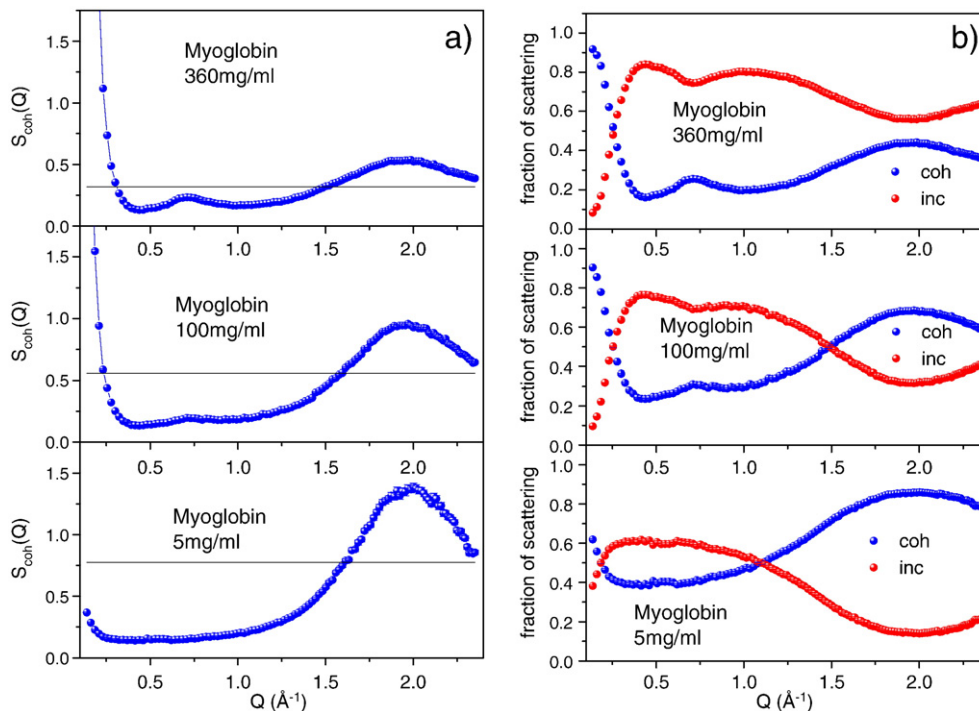


**Fig. 2.** (a) Coherent structure factors and (b)  $Q$ -dependent fractions of coherent and incoherent scattering events extracted from the DNS data on myoglobin powders at different  $\text{D}_2\text{O}$  hydration levels (see Table 1). The straight horizontal lines in (a) represent for each sample the value  $\sigma_{\text{coh}}/\sigma_{\text{tot}}$  presented in Table 1.

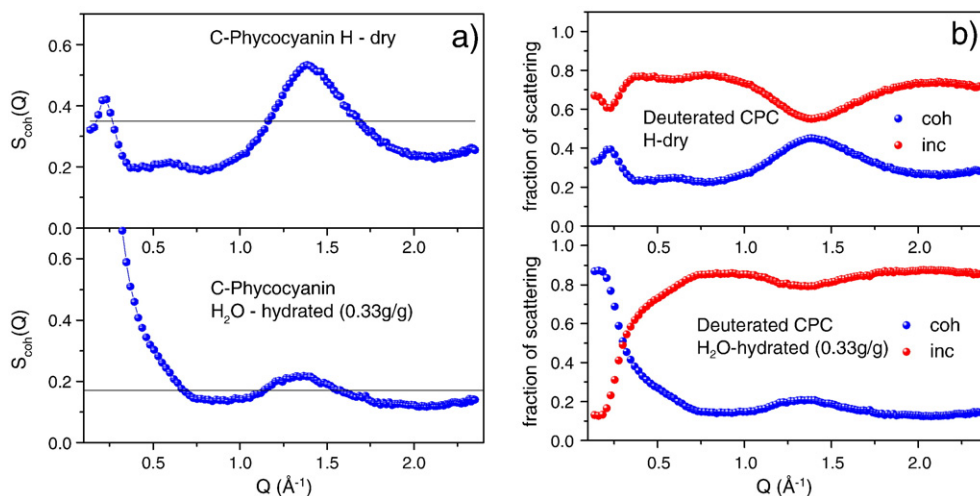
### 3.2. Powders of per-deuterated C-phycoyanin

Fig. 4 depicts the results, coherent structure factors (a) and  $Q$ -dependent fractions of coherent and incoherent scattering events (b), obtained for powders of per-deuterated C-phycoyanin (see Table 1).

The maxima and minima observed in the structure factor of the dry sample (Fig. 4a, top), have bigger amplitude than the ones observed for the dry myoglobin sample due to the higher coherent scattering power of the per-deuterated sample (Table 1). These maxima and minima are consistent with previous results of structural investigations on amorphous per-deuterated C-phycoyanin [29]. As for the



**Fig. 3.** (a) Coherent structure factors and (b)  $Q$ -dependent fractions of coherent and incoherent scattering events extracted from the DNS data on three exemplary solutions of myoglobin in  $\text{D}_2\text{O}$ . The straight horizontal lines in (a) represent for each sample the value  $\sigma_{\text{coh}}/\sigma_{\text{tot}}$  presented in Table 1.



**Fig. 4.** (a) Coherent structure factors and (b)  $Q$ -dependent fractions of coherent and incoherent scattering events extracted from the DNS data on the deuterated C-phycoyanin powders. The straight horizontal lines in (a) represent for each sample the value  $\sigma_{\text{coh}}/\sigma_{\text{tot}}$  presented in Table 1.

structure factor of the hydrated powder, a significant reduction in the amplitude of the coherent oscillations above  $0.60 \text{ \AA}^{-1}$  is observed, due to the overall reduction in the coherent scattering power of the sample. At the same time, an increase of coherent scattering is observed below  $0.60 \text{ \AA}^{-1}$  due to the formation of a hydration layer of H<sub>2</sub>O molecules around the protein of scattering power significantly different from that of the protein.

Concerning the  $Q$ -dependent fractions of coherent and incoherent scattering events, displayed in Fig. 4b, three aspects are worth mentioning: First, the dry powder scatters mainly incoherently over the entire  $Q$ -range investigated, with the incoherent term representing between 55% and 77% of the scattering, depending on the particular  $Q$ -value considered (Fig. 4b, top). This implies that quasielastic neutron scattering experiments performed on such a sample access simultaneously self-diffusion of the protein labile hydrogen atoms, as well as collective dynamics of the protein atoms.

Second, the hydrated powder also scatters mainly incoherently above a certain  $Q$ -value, the fraction of incoherent scattering events following the expected  $\sigma_{\text{inc}}/\sigma_{\text{tot}}$  value, with some oscillations that may be considered of small amplitude (the fraction of incoherent scattering varying between 88% and 80% of the signal for  $Q > 0.60 \text{ \AA}^{-1}$  – Fig. 4b, bottom). It should be noted, however, that only about 70% of the incoherent scattering will originate from the hydrogen atoms in the hydration layer of the protein, the remaining 30% originating from the labile hydrogen atoms present in the protein (as can be easily seen from the sample atomic composition presented in Table 1). This implies that, in fact, only about 55–60% of the total scattering from this sample will actually represent incoherent scattering from the hydration layer of the protein. Great caution should, therefore, be exercised when interpreting the results from dynamic neutron scattering experiments on such samples, as the scattering signal will contain information on at least three distinct dynamical processes: self-diffusion of the hydration water molecules, single particle fluctuations of the labile atoms of the protein and the collective dynamics of the other protein atoms.

Third, for the hydrated sample and for  $Q$ -values below  $0.60 \text{ \AA}^{-1}$ , the coherent term will increasingly dominate the scattering signal with the crossover from mainly incoherent scattering to mainly coherent scattering occurring at  $0.30 \text{ \AA}^{-1}$ , the coherent term even reaching a level of 87% of the signal at  $0.16 \text{ \AA}^{-1}$  (Fig. 4b, bottom). A change from an 80% coherent scatterer at  $0.20 \text{ \AA}^{-1}$  to an 80% incoherent scatterer at  $0.60 \text{ \AA}^{-1}$ , must necessarily be taken into account for the proper interpretation of any dynamic neutron scattering results collected over this  $Q$ -range, especially if  $Q$ -dependent effects are considered.

#### 4. Conclusions

Polarization analysis was successfully used to separate experimentally the coherent and incoherent contributions to the static scattering functions of different protein samples, over a wide range of  $Q$ -values extending from the small-angle region ( $0.006 < Q < 0.04 \text{ \AA}^{-1}$ ) to the intermediate and wide-angle regions (up to  $2.35 \text{ \AA}^{-1}$ ). Thereby, not only coherent structure factors have been directly obtained from the experiment over a  $Q$ -region where significant incoherent backgrounds are already present, but also quantitative information was obtained on the  $Q$ -dependent fraction of coherent to incoherent scattering, over the  $Q$ -region usually accessible on backscattering and time-of-flight instruments. This latter information is of special relevance to the community investigating protein and protein hydration water dynamics by quasielastic neutron scattering methods, as it provides a means for a more accurate interpretation of the results obtained at instruments measuring the total dynamic scattering function.

The results obtained show, for all the samples investigated, that even though for  $Q$ -values higher than  $0.20$ – $0.30 \text{ \AA}^{-1}$  the coherent scattering term does fall below the incoherent term, the situation of a clear predominance of the incoherent term over the coherent term, to the extent that the latter can be neglected, is never observed. The two terms even alternate roles at higher  $Q$ -values in the case of the aqueous solutions investigated.

The  $Q$ -dependent fractions of coherent and incoherent scattering oscillate around the values given by  $\sigma_{\text{coh}}/\sigma_{\text{tot}}$  and  $\sigma_{\text{inc}}/\sigma_{\text{tot}}$  with amplitudes that increase with the value of  $\sigma_{\text{coh}}/\sigma_{\text{tot}}$ . Hence, whereas for some samples (say with  $\sigma_{\text{coh}}/\sigma_{\text{tot}} \leq 0.20$ ) and for  $Q$ -values higher than a certain threshold (determined to be  $0.35 \text{ \AA}^{-1}$  in the case of the protonated myoglobin samples and  $0.60 \text{ \AA}^{-1}$  in the case of the per-deuterated C-phycoyanin samples), it might still be possible to assume that the total scattering signal is composed by a fairly  $Q$ -independent mixture of coherent and incoherent scattering (of fractions given by  $\sigma_{\text{coh}}/\sigma_{\text{tot}}$  and  $\sigma_{\text{inc}}/\sigma_{\text{tot}}$ ), for other samples of higher coherent scattering power this assumption no longer holds, with the  $Q$ -dependent fractions of coherent and incoherent scattering changing significantly over the entire  $Q$ -range investigated. Such an assumption also does not hold for  $Q$ -values below the mentioned thresholds, since there the coherent scattering will increasingly dominate with decreasing  $Q$ -values.

Hence any interpretation of the results of dynamic neutron scattering experiments performed exploring the  $Q$ -values above  $0.05 \text{ \AA}^{-1}$  should bear in mind that a mixture of coherent and

incoherent scattering is being observed, as well as the possible variation of importance of the two contributions, whenever  $Q$ -dependent effects are being analyzed. As an example, we would like to mention the crossover from predominantly incoherent scattering to predominantly coherent scattering observed for many protein samples when  $Q$ -decreases below  $\approx 0.30 \text{ \AA}^{-1}$ . This crossover should provide an interesting means for the analysis of the transition from a scattering function dominated by self-diffusion to a scattering function dominated by collective diffusion. On the other hand, ignoring the presence of this transition and analyzing the data in this  $Q$ -range assuming being in the presence of just incoherent scattering, would probably lead to incorrect interpretations of the  $Q$ -dependent effects observed.

At last we would like to mention, that a natural step forward from these investigations would be to perform directly quasielastic scattering experiments with polarization analysis. This would allow to experimentally determine, at the same  $Q$ -value, the differences between self and collective dynamics. It should also be emphasized that the measurements discussed in this paper are static scattering measurements. Hence the results obtained represent the proportions of coherent and incoherent scattering at  $t = 0$  (at the starting point of the intermediate scattering function). How these proportions may vary in the time domain depends on the coherent and incoherent relaxation processes at the origin of the quasielastic scattering signal and how different their characteristic times may be. Also for this reason quasielastic measurements with polarization analysis would be of great interest.

### Acknowledgments

Dr. Sergey Masalovich from the  $^3\text{He}$  Station “Helios” at the FRM II is acknowledged for his friendly assistance during the experiments involving polarized  $^3\text{He}$  cells at MIRA and discussions afterwards. Continuous incentive by Prof. Winfried Petry as scientific director of the FRM II is also gratefully acknowledged.

A. M. Gaspar acknowledges the support given by Fundação para a Ciência e Tecnologia in the form of a post-doc grant SFRH/BDP/17571/2004. The project was further supported by a grant of the Deutsche Forschungsgemeinschaft SFB 533.

### References

- [1] P.A. Egelstaff (Ed.), Thermal Neutron Scattering, Academic Press Inc., 1965.
- [2] G.L. Squires, Introduction to the Theory of Thermal Neutron Scattering, Dover Publications Inc, 1978.
- [3] K. Sköld and D.L. Price in Neutron scattering, K. Sköld and D.L. Price (editors),

- volume 23 part A of Methods of Experimental Physics, chapter 1, Introduction to neutron scattering, Academic Press Inc, (1986).
- [4] M. Bee, Quasielastic Neutron Scattering: Principles and Applications in Solid State Chemistry, Biology and Materials Science, Adam Hilger, 1988.
- [5] G. Hohler (Ed.), Quasielastic Neutron Scattering for the Investigation of Diffusive Motions in Solids and Liquids, Volume 64 of Springer Tracts in Modern Physics, Springer-Verlag, 1972.
- [6] K. Sköld, Small energy transfer scattering of cold neutrons from liquid argon, Phys. Rev. Lett. 19 (1967) 1023–1025.
- [7] R.M. Moon, T. Riste, W.C. Köhler, Polarization analysis of thermal-neutron scattering, Phys. Rev. 181 (1969) 920–931.
- [8] O. Schärpf, Polarization analysis techniques for quasielastic neutron scattering, Physica B 182 (1982) 376–388.
- [9] W. Gavin Williams, Polarized Neutrons, Carendon Press Oxford, 1988.
- [10] J.C. Dore, J.H. Clarke, J.T. Wenzel, Separation of coherent and spin-incoherent neutron scattering by polarization analysis, Nucl. Instrum. Meth. 138 (1976) 317–319.
- [11] B.J. Gabrys, Applications of polarized neutrons to non-magnetic materials, Physica B 267–268 (1999) 122–130.
- [12] T.R. Gentile, G.L. Jones, A.K. Thompson, J. Barker, C.J. Glinka, B. Hammouda, J.W. Lynn, SANS polarization analysis with nuclear-spin-polarized  $^3\text{He}$ , J. Appl. Cryst. 33 (2000) 771–774.
- [13] B.J. Gabrys, W. Zajac, O. Schärpf, QENS from “soft” systems: why use polarised neutrons? Physica B 301 (2001) 69–77.
- [14] J. Fitter, T. Gutberlet, J. Katsaras (Eds.), Neutron Scattering in Biology: Techniques and Applications, Springer Biological Physics Series, 2006.
- [15] J.H. Roh, J.E. Curtis, S. Azzam, V.N. Novikov, I. Peral, Z. Chowdhuri, R.B. Gregory, A.P. Sokolov, Influence of hydration on the dynamics of lysozyme, Biophys. J. 91 (2006) 2573–2588.
- [16] R. Georgii, et al., webpage of MIRA, <http://www.frm2.tum.de/en/science/diffractometer/mira/index.html>.
- [17] Y. Su, et al., webpage of DNS, [http://www.jcns.info/jcns\\_dns](http://www.jcns.info/jcns_dns).
- [18] V.F. Sears, Neutron scattering lengths and cross sections of the elements and their isotopes, Neutron News 3 (1992) 29–37.
- [19] J. Wuttke, FRIDA (fast reliable inelastic data analysis), <http://sourceforge.net/projects/frida>.
- [20] R. Zorn, Multiple scattering correction of polarized neutron diffraction data, Nucl. Instrum. Methods Phys. Res. A 479 (2002) 568–584.
- [21] J. Wuttke, Data reduction for quasielastic neutron scattering, ILL internal report 91WU08T, (1991).
- [22] M. Bee, Quasielastic Neutron Scattering: Principles and Applications in Solid State Chemistry, Biology and Materials Science, Adam Hilger, 1988 appendix of chap 4.
- [23] O. Schärpf, Experience with spin analysis on a time-of-flight multidetector scattering instrument. In Neutron scattering in the ‘nineties’, Proceedings of the IAEA Conference, Jülich (1985) 85–97.
- [24] B. Gabrys, O. Schärpf, Scattering from polymers using polarized neutrons: a new development, Physica B 180 & 181 (1992) 495–498.
- [25] Martin Diehl, Neutronen-Kleinwinkelstreuexperimente zur Untersuchung der Struktur hochkonzentrierter Myoglobinlösungen, Diploma thesis (1994), Technische Universität München.
- [26] M. Hirai, H. Iwase, T. Hayakawa, K. Miura, K. Inoue, Structural hierarchy of several proteins observed by wide-angle solution scattering, J. Synchrotron Rad. 9 (2002) 202–205.
- [27] F. Franks (Ed.), Water a Comprehensive Treatise: the Physics and Physical Chemistry of Water, volume 1, Plenum Press, 1972.
- [28] L. Bosio, J. Teixeira, M.-C. Bellissent-Funel, Enhanced density fluctuations in water analyzed by neutron scattering, Phys. Rev. A 39 (1989) 6612–6613.
- [29] M.-C. Bellissent-Funel, J. Lal, K.F. Bradley, S.H. Chen, Neutron structure factors of in-vivo deuterated amorphous protein C-phycoyanin, Biophys. J. 64 (1993) 1542–1549.